Model exact low-lying states and spin dynamics in ferric wheels: Fe_6 to Fe_{12}

Indranil Rudra,[1] S. Ramasesha,[1] and Diptiman Sen[2]
[1]*Solid State and Structural Chemistry Unit, Indian Institute of Science, Bangalore 560 012, India*
[2]*Centre for Theoretical Studies, Indian Institute of Science, Bangalore 560 012, India*
(Received 18 January 2002; revised manuscript received 12 April 2002; published 19 July 2002)

Using an efficient numerical scheme that exploits spatial symmetries and spin parity, we have obtained the exact low-lying eigenstates of exchange Hamiltonians for ferric wheels up to Fe_{12}. The largest calculation involves the Fe_{12} ring which spans a Hilbert space dimension of about 145×10^6 for the $M_S=0$ subspace. Our calculated gaps from the singlet ground state to the excited triplet state agree well with the experimentally measured values. Study of the static structure factor shows that the ground state is spontaneously dimerized for ferric wheels. The spin states of ferric wheels can be viewed as quantized states of a rigid rotor with the gap between the ground and first excited states defining the inverse of the moment of inertia. We have studied the quantum dynamics of Fe_{10} as a representative of ferric wheels. We use the low-lying states of Fe_{10} to solve exactly the time-dependent Schrödinger equation and find the magnetization of the molecule in the presence of an alternating magnetic field at zero temperature. We observe a nontrivial oscillation of the magnetization which is dependent on the amplitude of the ac field. We have also studied the torque response of Fe_{12} as a function of a magnetic field, which clearly shows spin-state crossover.

DOI: 10.1103/PhysRevB.66.014441 PACS number(s): 75.45.+j, 75.50.Xx, 75.60.Ej

I. INTRODUCTION

In recent years polyoxometalates which are practical realizations of nanomagnets have become an area of intense research because of their enormous variety of structures and fascinating magnetic properties. A particular aesthetic class is that of the ring-shaped iron(III) compounds denoted as molecular ferric wheels. The decanuclear wheel Fe_{10} synthesized by Taft *et al.*[1] may be regarded as a prototype of this class. Meanwhile, synthesis of ferric wheels with 6, 8, 12, and 18 sites have also been reported.[2] These materials have a dominant antiferromagnetic coupling between the Fe(III) spins and a singlet ground state. The magnetic properties of such nanoscopic molecules result from the interplay of superexchange interactions between the atomic spins, dipolar coupling of the local moments, and on-site anisotropies arising from ligand configurations. The emergence of ferric wheels has led to a renewed interest in the properties of the Heisenberg chain, especially for large spin values. In 1964 Bonner and Fisher used a classical treatment,[3] in which spin quantization is absent, to study the properties of the Heisenberg Hamiltonian and found analytical solutions for the thermodynamic properties of the system. Numerous quantum mechanical calculations have been made for the Heisenberg Hamiltonian, mostly for spin-1/2 chains. Calculations for larger S became more interesting after Haldane's conjecture[4] regarding the presence of an energy gap in the excitation spectrum from the ground state for integer S chains.

To fit the experimental temperature dependence of the magnetic susceptibility data for Fe_{10}, Taft *et al.* adopted a classical spin treatment to obtain the value of the exchange interaction parameter J. But below 50 K this treatment fails. Ferric wheels with $S=5/2$ and system size of up to eight sites have been treated exactly using the irreducible tensor operator technique[5] with the aid of point group symmetry as well as by using the invariance of the spin Hamiltonian with regard to interchange of spin sites.[6] Recently there have been theoretical studies to explain the low-temperature magnetic susceptibility data of Fe_{10}.[7] The magnetization of ferric wheels exhibit a steplike field dependence at low temperature due to the occurrence of field-induced ground-state level crossing, a spectacular manifestation of quantum size effects in these nanomagnets.[1,8] There have been NMR and specific heat studies of these ferric wheels to investigate the energy level structure.[9,10] In appropriate parameter regime these ring systems are considered to be candidates for the observation of macroscopic quantum phenomena,[11] in the form of quantum coherent tunneling of the Néel vector.[12] To understand these low-temperature properties of ferric wheels in detail we need to know the low-lying eigenvalue spectrum for these systems. It is also of interest to compare and contrast the zero-temperature density of states of $S=5/2$ rings with that of the exactly known $S=1/2$ chain. In this paper we have used spin parity together with rotational symmetry of the ferric wheels to obtain the low-lying eigenvalue spectrum for rings with 6, 8, 10, and 12 spin-5/2 sites. The dispersion spectrum reveals interesting features. There have been recent reports of solving the low-lying eigenspectrum of Fe_{10} using the density matrix renormalization group method.[13] To the best of our knowledge, our's is the first study of ferric wheels using exact methods up to a ring size of 12, $S=5/2$ iron(III) ions.

We have also studied the quantum spin dynamics of ferric wheels in the presence of an alternating field after setting up the Hamiltonian matrix in the subspace of low-lying states. This Hamiltonian includes multipolar spin-spin interaction terms besides a time varying magnetic field (Zeeman term). We have then evolved an initial state, which is taken to be the ground state with a specific value of M_S (the z component of the total spin) in the absence of a magnetic field, by using the time-dependent formulation of the problem in the restricted subspace. We observe a nontrivial oscillation of the magnetization whose frequency depends on the amplitude of

the alternating field. This phenomenon is very similar to what has been observed in case of uniaxial magnets.[14]

II. MODEL HAMILTONIAN AND COMPUTATIONAL DETAILS

A. Symmetry adaptation of correlated states

The full symmetry of electronic states is of central interest in quantum theory. Since nonrelativistic Hamiltonians $\hat{H}$ do not depend explicitly on spin, molecular eigenstates can be labeled by the total spin S and the appropriate irreducible representation of the point group. The model Hamiltonian employed in this study is the isotropic exchange Hamiltonian involving an exchange interaction between nearest neighbors,

$$\hat{H}=\sum_{\langle ij\rangle} J_{ij}\hat{s}_i\cdot\hat{s}_j, \tag{1}$$

where the exchange interaction J_{ij} takes the values dictated by experimental studies of the structure and magnetic properties. For Fe_6, the J value depends on the central alkali-metal atom; for Na: Fe_6, $J=32.77$ K, whereas for Li :Fe_6 $J=20.83$ K. In Fe_8, Fe_{10}, and Fe_{12}, J is 22 K, 15.56 K, and 31.97 K, respectively.[15]

The total dimensionality of the Fock space of the ferric wheel is given by

$$D_F=\prod_1^n (2S_i+1), \tag{2}$$

where n is the total number of spins in the wheel and S_i is the spin on each ion. In the case of Fe_{10}, there are ten iron(III) ions with the dimensionality of the Fock space being 60 466 176. In the case of Fe_{12}, which we have solved exactly, this dimension is 2 176 782 336.

Specializing to a given total M_S leads to Hilbert space dimensionalities which are lower than the Fock space dimensionality. In the case of the Fe_{12} cluster, the $M_S=0$ space has a dimensionality of about 145×10^6 (144 840 476). The major challenge in an exact computation of the eigenvalues and properties of these spin clusters lies in handling such large bases and the associated matrices. While the dimensions look overwhelming, the matrices that represent the operators in these spaces are rather sparse. Usually, the number of nonzero elements in a row is of the order of the number of exchange constants in the Hamiltonian. This sparseness of the matrices allows one to handle fairly large systems. However, in the case of spin problems, generating the bases states and using the symmetries of the problem is nontrivial.

The isotropic exchange Hamiltonians conserve total spin S besides the z component of the total spin M_S. Besides these symmetries, the geometry of the cluster also leads to spatial symmetries which can often be exploited. The simplest way of generating bases functions which conserve total spin is the valence bond (VB) method, which employs the Rumer-Pauling rule.[16] It is quite easy to generalize the Rumer-Pauling rules to a cluster consisting of objects with different spins to obtain states with a desired total spin S. However, setting up the Hamiltonian matrix in such a basis can be computationally intensive since the exchange operators operating on a ''legal'' VB diagram (a diagram that obeys Rumer-Pauling rules) could lead to ''illegal'' VB diagrams, and resolving these illegal VB diagrams into legal diagrams would present the major bottleneck. Indeed, the same difficulty is encountered when spatial symmetry operators operate on a VB function. Thus, the extended VB methods are not favored whenever one wishes to apply it to a motley collection of spins or when one wishes to exploit some general spatial symmetries that may exist in the cluster.[17]

It is advantageous to partition the spaces into different total spin spaces because of the usually small energy gaps between total spin states which differ in S by unity. To avoid the difficulties involved in working with total spin eigenfunctions, we exploit parity symmetry in the systems. The parity operation involves changing the z component of all the spins in the cluster from M_{S_i} to $-M_{S_i}$. There is a phase factor associated with this operation given by $(-1)^{S_{tot}+\Sigma_i S_i}$. The isotropic exchange operator remains invariant under this operation. If this symmetry is employed in the $M_S=0$ subspace, the subspace is divided into ''even'' and ''odd'' parity spaces depending upon the sign of the character under the irreducible representation of the parity group. The space which corresponds to even (odd) total spin we call the even (odd) parity space. Thus, employing parity allows partial spin symmetry adaptation which separates successive total spin spaces, without introducing the complications encountered in the VB bases. However, the VB method can lead to complete factorization of the spin space leading to smaller complete subspaces.

In the ferric wheels, besides spin symmetries, there also exist spatial symmetries. The topology of the exchange interaction leads to a C_n point group symmetry, where n is the number of iron ions in the ring. Hence, Fe_6, Fe_8, Fe_{10}, and Fe_{12} will have C_6, C_8, C_{10}, and C_{12} symmetry, respectively. It should be mentioned that among these ferric wheels only Fe_{10} strictly has a tenfold rotational symmetry; the rest of them only approximately have the above-mentioned symmetry. For computational advantage we have assumed rotational symmetry for all the ferric wheels. This point group appears at first site to present difficulties because the characters in the irreducible representation are in some cases complex which could lead to complex bases functions. This, however, can be avoided by recognizing that in the C_n group, states with wave vectors k and $-k$ are degenerate. We can therefore construct a linear combination of the k and $-k$ states which is real. The symmetry representations in the C_n group would then correspond to the labels A, B, and E, with the characters in the E representation given by $2\cos(rk)$ under the symmetry operation C_n^r, with $k=\pi/n$. The parity operation commutes with the spatial symmetry operations, and the full point group of the system would then correspond to the direct product of the two groups. Since both parity and spatial symmetries can be easily incorporated in a constant M_S basis, we do not encounter the difficulties endemic to the VB theory.

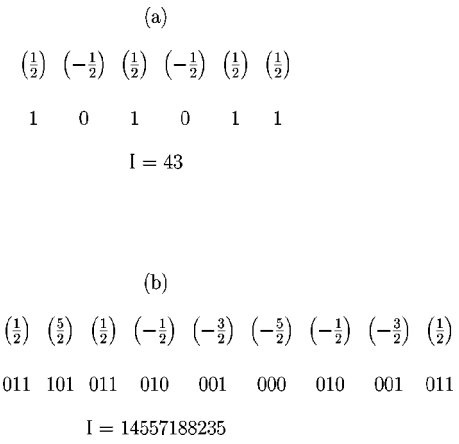

FIG. 1. Representative $M_s=0$ states in (a) six-spin-$\frac{1}{2}$ cluster, (b) Fe_{12} wheel with all the sites having spin $S=\frac{5}{2}$. Numbers in parentheses correspond to the M_s value at the site. The bit representation as well as the integer value is given just below the diagrams.

The generation of the complete basis in a given Hilbert space requires a simple representation of a state on the computer. This is achieved by associating with every state a unique integer. In this integer, we associate n_i bits with spin s_i, such that n_i is the smallest integer for which $2^{n_i} \geqslant (2s_i+1)$. In the integer that represents the state of the cluster, we ensure that these n_i bits do not take values which lead to the n_i bit integer value exceeding $(2s_i+1)$. For each of the allowed bit states of the n_i bit integer, we associate an M_{S_i} value between $-s_i$ and s_i. For a spin cluster of n spins, we scan all integers of bit length $N=\Sigma_{i=1}^{n} n_i$ and verify if it represents a basis state with the desired M_S value. In Fig. 1, we show a few basis functions with specified M_s values for some typical ferric wheels along with their bit representations and the corresponding integers. The generation of the bases states is usually a very fast step, computationally. Generating the basis as an ordered sequence of integers that represent them also allows for a rapid generation of the Hamiltonian matrix elements as will be seen later.

The symmetrization of the basis by incorporating parity and spatial symmetries involves operating on the constant $M_S=0$ basis by the symmetry operators. Since the spatial symmetry operators permute the positions of equivalent spins, every spatial symmetry operator operating on a basis function generates another basis function. Every symmetry operator can be represented by a corresponding vector whose ith entry gives the state that results from operating on the ith state by the chosen operator. This is also true for the parity operator, in the $M_S=0$ subspace.

The first step in constructing symmetry-adapted linear combinations is to represent the symmetry operators in the chosen basis as matrices. In our case, the symmetry operators are such that a symmetry operation by any operator on a basis state leads to a resultant which is a single basis state. Thus all our symmetry operators can be represented as vectors; the entry in position i gives the index of the basis function generated by the symmetry operation on the basis state i. Since the basis is very large, it is prohibitive to store and manipulate the full basis together with all the associated symmetry vectors. To avoid these difficulties, we have constructed the symmetry matrices in small invariant subspaces. These invariant subspaces are obtained by sequentially choosing a state and operating on it by all the symmetry operators. This gives rise to a set of states on which we again operate by all the symmetry operators and continue this process until no new basis states are generated. The collection of all these basis states resulting at the end of this process is the invariant subspace. We can set up symmetry combinations of the basis states in each of the invariant subspaces independently. The symmetry combinations can now be obtained operating on each state by the group-theoretic projection operator

$$\hat{P}_{\Gamma_i}=\frac{1}{h}\sum_R \chi_{\Gamma_i}(R)\hat{R} \tag{3}$$

on each of the basis states of the invariant subspace. Here Γ_i is the ith irreducible representation, $\hat{R}$ is the symmetry operation of the group, and $\chi_{\Gamma_i}(R)$ is the character under $\hat{R}$ in the irreducible representation Γ_i. This process is repeated with the next basis state that has not appeared in any of the invariant subspaces already constructed. The process comes to an end when all the basis states have appeared in any one of the invariant subspaces.

The resulting symmetrized basis is usually overcomplete in each of the invariant subspaces. The linear dependences can be eliminated by a Gram-Schmidt orthonormalization procedure. However, in most cases, ensuring that a given basis function does not appear more than once in a symmetrized basis is sufficient to guarantee linear independence and weed out the linearly dependent states. A good check of the procedure is to ensure that the dimensionality of the symmetrized space in the invariant subspace agrees with that calculated from the traces of the reducible representation obtained from the matrices corresponding to the symmetry operators in the chosen invariant subspace. Besides, the sum of the dimensionalities of the symmetrized spaces should correspond to the dimensionality of the unsymmetrized invariant subspace in each of these subspaces.

The generation of the Hamiltonian matrix is rather straightforward and involves operating with the Hamiltonian operator on the symmetry-adapted basis. This results in the matrix **SH**, where **S** is the symmetrization matrix representing the operator $\hat{P}_{\Gamma_i}$, and **H** is the matrix whose elements h_{ij} are defined by

$$\hat{H}|i\rangle=\sum_j h_{ij}|j\rangle. \tag{4}$$

The states $\{i\}$ correspond to the unsymmetrized basis functions. The Hamiltonian matrix in the symmetrized basis is obtained by right multiplying the matrix **SH** by $\mathbf{S}^{\dagger}$. The resulting symmetric Hamiltonian matrix is stored in the sparse matrix form, and the matrix eigenvalue problem is solved using the Davidson algorithm.[18]

The computation of the properties is easily done by transforming the eigenstate in the symmetrized basis into that in the unsymmetrized basis. Since the operation by any combi-

nation of spin operators on the unsymmetrized basis can be carried out, all relevant static properties in different eigenstates can be obtained in a straightforward manner.

B. Quantum spin dynamics

We have studied the dynamics in ferric wheels by setting up the Hamiltonian matrix in the desired M_S space, which in all cases is restricted to $M_S=0$, 1, and 2. In each subspace we have obtained a few low-lying states using the Davidson algorithm.[18] We have also calculated the spin-spin correlation functions in each of the states. Using the spin-spin correlation functions, we have computed the expectation value of the S^2_total operator, from which we have identified the total spin of the state. We observe from the eigenvalue spectrum of all the ferric wheels that the ground state and the first excited state are spin-singlet ($S=0$) and -triplet ($S=1$) states, respectively, in accordance with the Lieb-Schultz-Mattis theorem.[19] These states belong to different spatial symmetry subspaces as well as different parity subspaces. So they will not mix unless there is a perturbation which spoils both the C_{10} symmetry of the molecule and the parity. We also notice that the first (triplet) and the second (quintet) excited states again fall into different symmetry subspaces. This is true in all the ferric wheels we have studied.

To study quantum dynamics we have considered the following Hamiltonian:[20]

$$\hat{H}=E_s-D\hat{S}^2_{z,\text{total}}+c(\hat{S}^2_{x,\text{total}}-\hat{S}^2_{y,\text{total}})-gh(t)\hat{S}_{z,\text{total}}. \quad (5)$$

Here D is the quadratic anisotropy factor, g is the Landé g factors for the iron(III) spin, respectively, and $h(t)$ is the time-dependent magnetic field, expressed as $h(t)=H_0\cos(\omega t)$, where ω is the frequency at which the field is ramped and H_0 is the amplitude of the field. We have chosen $D=8.8\times10^{-3}$ and $c=10^{-3}$ (in units of J) in accordance with the experimental values for Fe_{10}. We take $g=2.0$. The constants E_s in Eq. (5) correspond to the lowest energies obtained from Eq. (1). The second-order anisotropy term allows transitions between states with $\Delta M_S=\pm2$. Both the second and third terms in Eq. (5) arise due to the magneto-crystalline anisotropy. The exact form of the anisotropy in ferric wheels is not very well established. We have included anisotropy terms only up to second order in the spin variables. The anisotropy in the plane can be formed artificially, e.g., by means of external electric or magnetic fields, pressure, or using an anisotropic substrate.[20]

To observe spin dynamics, we begin with the initial state $|S=1,M_S=-1\rangle$, and then apply an external field in Eq. (5) of the form

$$h(t)=H_0\cos(\omega t). \quad (6)$$

The Hamiltonian in Eq. (5) does not allow the mixing of the ground state (singlet) and the first excited state (triplet) in Fe_{10} because of the symmetry reasons already mentioned. Therefore, to observe the dynamics in the magnetization, we have chosen the above initial state.[21] To study the evolution of the magnetization as a function of the applied oscillatory field, we start in the initial state at time $t=0$ and time-evolve the state in small steps of $\Delta t=0.01$ ($\hbar/J$) by solving the time-dependent Schrödinger equation

$$i\hbar\frac{d\psi}{dt}=\hat{H}(t)\psi. \quad (7)$$

In actual practice, the state is time evolved according to the equation

$$\psi(t+\Delta t)=e^{-i\hat{H}(t+\Delta t/2)\Delta t/\hbar}\psi(t). \quad (8)$$

The evolution is carried out by explicit diagonalization of the Hamiltonian matrix $\mathbf{H}(t+\Delta t/2)$, and using the resulting eigenvalues and eigenvectors to evaluate the matrix of the time evolution operator $e^{-i\hat{H}(t+\Delta t/2)\Delta t/\hbar}$. We set up the Hamiltonian matrix for time evolution in the truncated basis of three states corresponding to total spin $S=1$. We repeatedly carry out the time evolution in small time steps of size Δt to obtain the time evolution over longer periods.

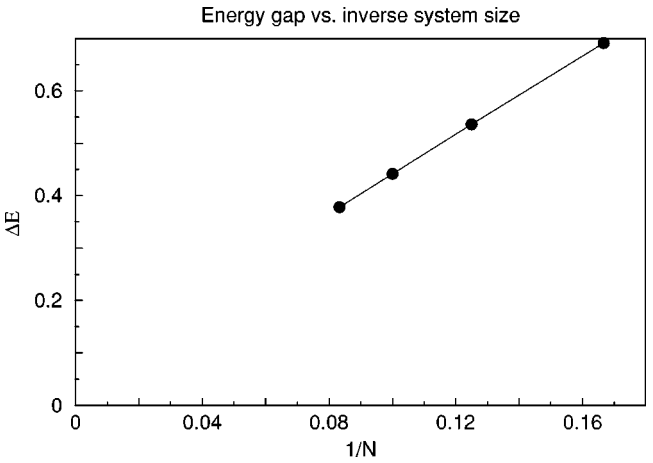

FIG. 2. Plot of ground-state energy (in units of J) vs inverse system size for ferric wheels up to Fe_{12}.

III. RESULTS AND DISCUSSION

A. Analysis of the low-lying spectrum

We have solved the exchange Hamiltonian [Eq. (1)] exactly using the method mentioned earlier to obtain the low-lying eigenvalue spectrum for 6-, 8-, 10-, and 12-site iron(III) rings. We find that the ground state and first, second, and third excited states are, respectively, singlet and triplet, quintet, and heptet for all ferric wheels. We notice that there is no accidental degeneracy between the energy levels belonging to different symmetry subspaces. The gap between the ground state and the first excited state is shown in Fig. 2 as a function of inverse ring size. According to the Haldane conjecture, the gap should extrapolate to zero. The extrapolated value, while small, is still finite, suggesting that in these rings finite-size effects are still at play at the ring sizes we have studied.

Using the exchange constants estimated for the different ring systems, we estimate the gap between the ground state and the first excited state to be 22.67 K, 11.81 K, and 6.88 K for $Na:Fe_6$, $Na:Fe_8$, $Na:Fe_{10}$, respectively. Our calculated

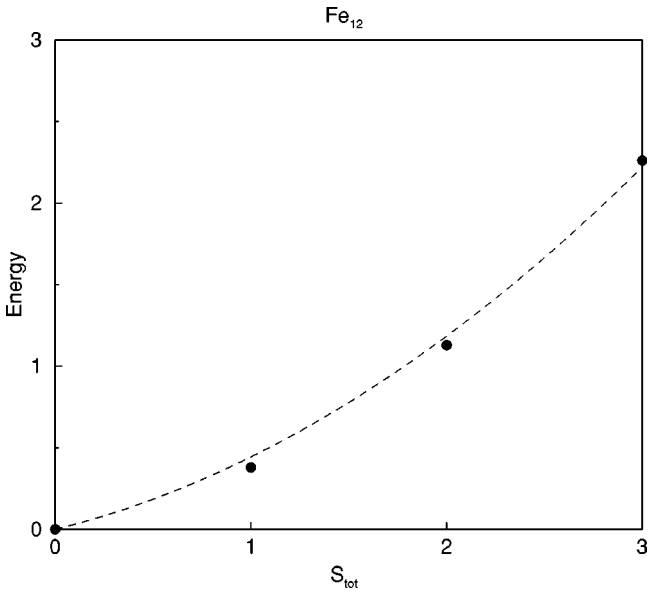

FIG. 3. Plot of lowest energy (in units of J) in every total spin sector vs the total spin (S_{tot}) in case of Fe_{12}. It clearly obeys the conjecture of Taft *et al.* (Ref. 1).

values compare very well with the experimental values, which are 22.0 K, 12.1 K, and 6.45 K for Na :Fe_6, Na:Fe_8, and Na:Fe_{10}, respectively.[15] This agreement shows that for all practical purposes ferric wheels can safely be assumed as rings neglecting the slight deviation from the exact circular geometry. Our calculated gap for Fe_{12} is 12.09 K, corresponding to the exchange constants predicted from experiments. However, an experimental estimate of this gap is lacking.

If we define δ_i to be the energy difference between the ith excited state and the ground state, we find from Fig. 3 that the following relationship is satisfied for the ferric wheels:

$$\delta_i = \frac{S_i(S_i+1)}{2} E_1, \tag{9}$$

where E_1 is the energy gap between the ground state and the first excited state. This indicates that the lowest spin state obeys the Lande interval rule, in agreement with the conjecture of Taft *et al.*[1] If we assume E_1 to be the inverse of the moment of inertia, then the above expression gives the rotational energy of a rigid rotor in a state with quantum number

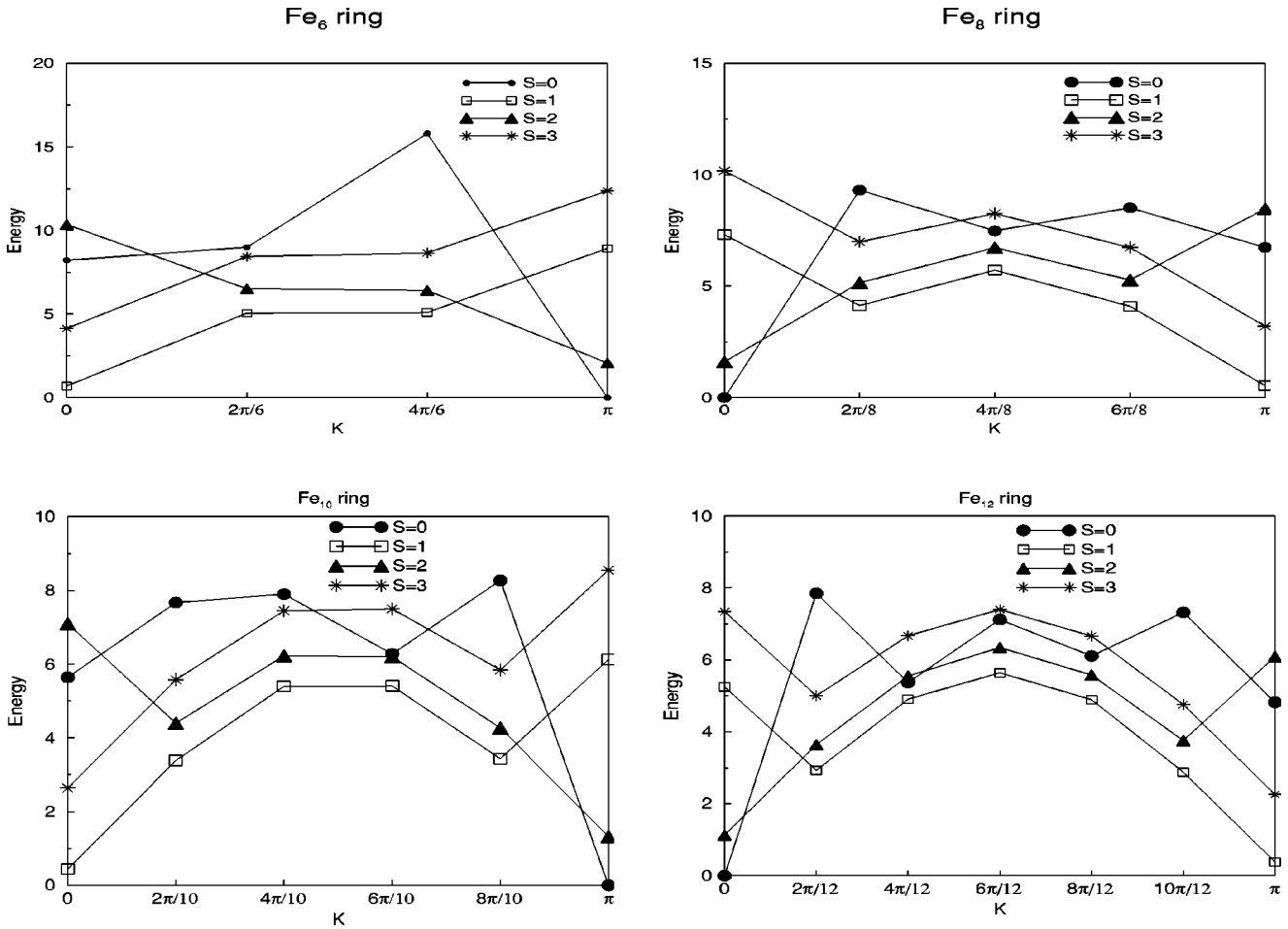

FIG. 4. Plot of energy (in units of J) vs momentum vector k for Fe_6, Fe_8, Fe_{10}, and Fe_{12}.

S_i. Thus, the spin states of ferric wheels can be viewed as the quantized states of a rigid rotor.

In Fig. 4 we have shown the dispersion spectrum of ferric wheels. The value of k corresponding to a wave function ψ can be defined as

$$T\psi = e^{ik}\psi, \tag{10}$$

where T is the translation operator which in the case of a ring rotates the ring by one lattice spacing. We have used the spatial C_n symmetry of the ferric wheels, which enables us to identify the value of k easily for a specified eigenfunction. We observe that the ground state switches between A^+ ($k=0$) and B^+ ($k=\pi$) subspace for systems with $N=4n$ and $N=4n+2$ spins, respectively. This was also observed by Mattheiss in the case of a spin-1/2 chain and can be understood from Marshall's sign rule. We find that, in the momentum (k) sector which contains the ground state, the lowest excitation is to a quintet state, while the lowest triplet excitation has a momentum which differs by π from the momentum of the ground state. In fact, for any momentum different from that of the ground state, the lowest excitation is a triplet state for all the four system sizes shown in Fig. 4; if this trend continues, we expect the triplet to be lower in energy than the quintet for any k value different from that of the ground state in the thermodynamic limit. Previous studies[22] on antiferromagnetic spin-1/2 Heisenberg chains show that the excitation spectrum is given by $\hbar\omega=(\pi/2)J|\sin k|$, where k is the wave vector of the excited states measured with respect to that of the ground state. Simple antiferromagnetic spin-wave theory, based on the use of the Holstein-Primakoff transformation for each sublattice, leads to the excitation spectrum (S is the magnitude of the individual spin S_i)

$$\hbar\omega = 2JS|\sin k|. \tag{11}$$

This relation is supposed to be correct for $S\to\infty$. We notice that the excitation spectrum for ferric wheels can be fitted to a $|\sin k|$ kind of function. Isolated data points in $k=0$ or $k=\pi$ deviate from the above sinusoidal function. This is a finite-size effect. In the thermodynamic limit of an infinite chain length, there is no distinction between chain lengths of $N=4n$ and $N=4n+2$, and the lowest-energy excitation will indeed be given by Eq. (11).

We have also calculated the spin-spin correlation function ($\langle S_i^z S_j^z\rangle$) of ferric wheels and Fourier-transformed it to find the structure factor

$$S(q) = \frac{1}{N^2}\sum_{m,n} e^{iq(m-n)}\langle S_m^z S_n^z\rangle, \tag{12}$$

where the allowed values of q are given by the cyclic boundary conditions. In Fig. 5, we have plotted the structure factor as a function of the wave vector q for different symmetry subspaces. In each part of the figure, we have plotted the structure factor for wheel sizes $N=6$, 8, 10, and 12. In all cases $S(q)$ shows a peak at $q=\pi$; the peak height increases slowly with wheel size. This is in agreement with the simple spin-wave analysis which shows that the peak height increases as $\ln(N)$. The peak height is the largest in the ground state. The peak heights in the three excited states are comparable to each other; a similar spin-wave analysis shows that the peak height $S(\pi)$ for the excited states is slightly smaller than the height in the ground state by a constant additive factor which is independent of the wheel size. The ground state is a Néel-ordered state; the peak at $S(\pi)$ signifies that the ground state is unstable to a spontaneous distortion with wave vector π.

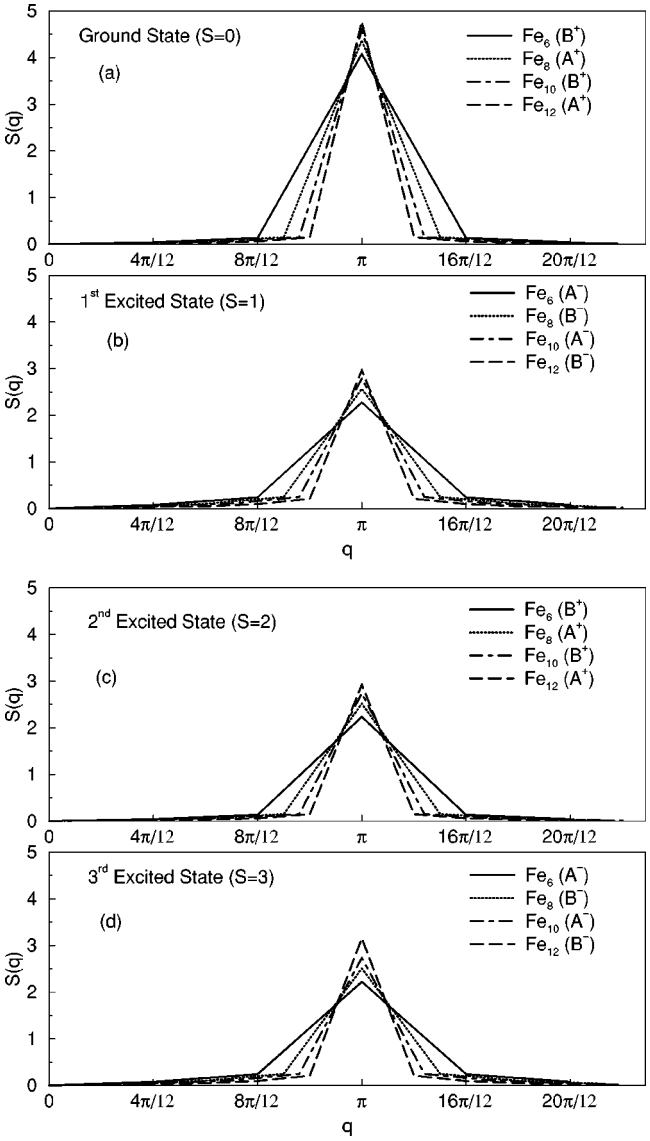

FIG. 5. Plot of static structure factor S_q for the ground and three lowest excited states for Fe_6, Fe_8, Fe_{10}, and Fe_{12}. Note that the spatial symmetry label for a given state alternates between $4n$ and $4n+2$ systems.

B. Evolution of magnetization in the presence of an ac field

We follow the evolution of the magnetization, beginning with the initial state $|S=1, M_S=-1\rangle$, in the presence of an axial ac magnetic field whose amplitude is varied. We have kept the frequency of the field fixed at $\omega=10^{-3}$. We calcu-

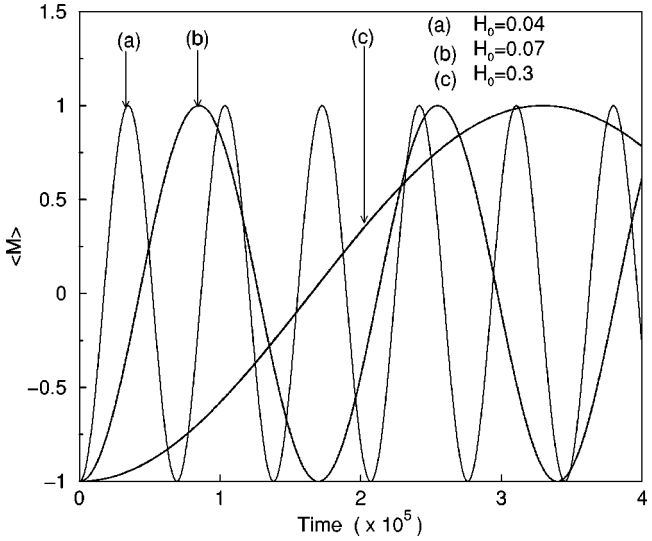

FIG. 6. Plot of evolution of magnetization in the presence of an alternating axial magnetic field H_0 (in units of $J/\hbar$) of three different amplitudes.

late the magnetization at each time step. When we draw a smooth curve for the time evolution over long time periods, we find a sinusoidal motion

$$M(t) \sim \cos(\Omega t), \tag{13}$$

which can be seen in Fig. 6. Unexpectedly, the frequency Ω of this sinusoidal motion does not correspond to an eigenfrequency of the system or to the period of the external field. When we change the amplitude H_0 of the field, the period of the magnetization changes, which is shown in Fig. 7. We find that the frequency of oscillation Ω becomes very small for some values of H_0, and then it increases again. A similar behavior is observed in the transverse field Ising model.[14] Indeed the physics of our model is similar to the model studied in Ref. 14 since the quadratic anisotropy factor $D \gg c$ in Eq. (5). The upper envelope of Ω as a function of H_0 can be empirically fitted to an inverse square root curve.

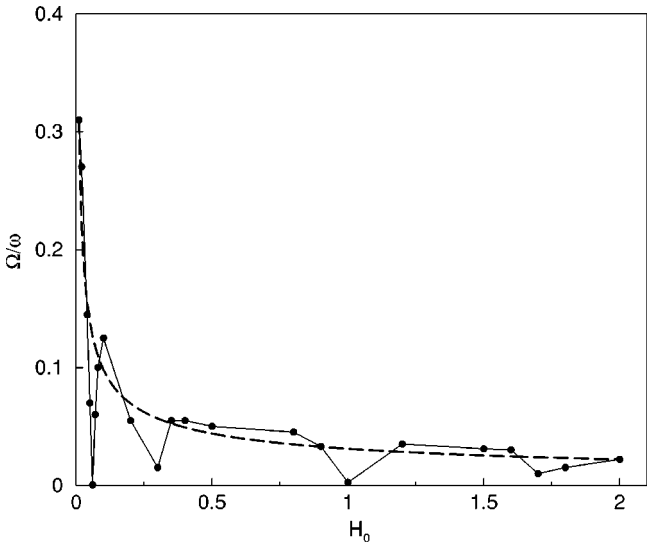

FIG. 7. Field amplitude (H_0) dependence of frequency Ω (defined in the text). The dotted line shows the inverse square root nature of the upper envelope.

For very small values of H_0, the magnetization oscillates with a frequency given by $\Delta E/\hbar$, where ΔE is the energy difference between the two approximate eigenstates $|S=1,M_S=-1\rangle$ and $|S=1,M_S=1\rangle$ of Eq. (5). Since $\Delta E \sim c$ [where c is the amplitude of the mixing term in Eq. (5)] and is comparable to $\omega = 10^{-3}$, the frequency of oscillation of $M(t)$, Ω, is also comparable to ω. Hence the ratio Ω/ω rapidly increases to 1 for small H_0.

For large values of H_0, the probability p of remaining in the ground state is small and, in fact, decreases as $1/H_0$.[14] Thus we have a nonadiabatic situation in which the state and its magnetization remain unchanged with a probability $1-p$ which is close to 1. One can then show that the magne-

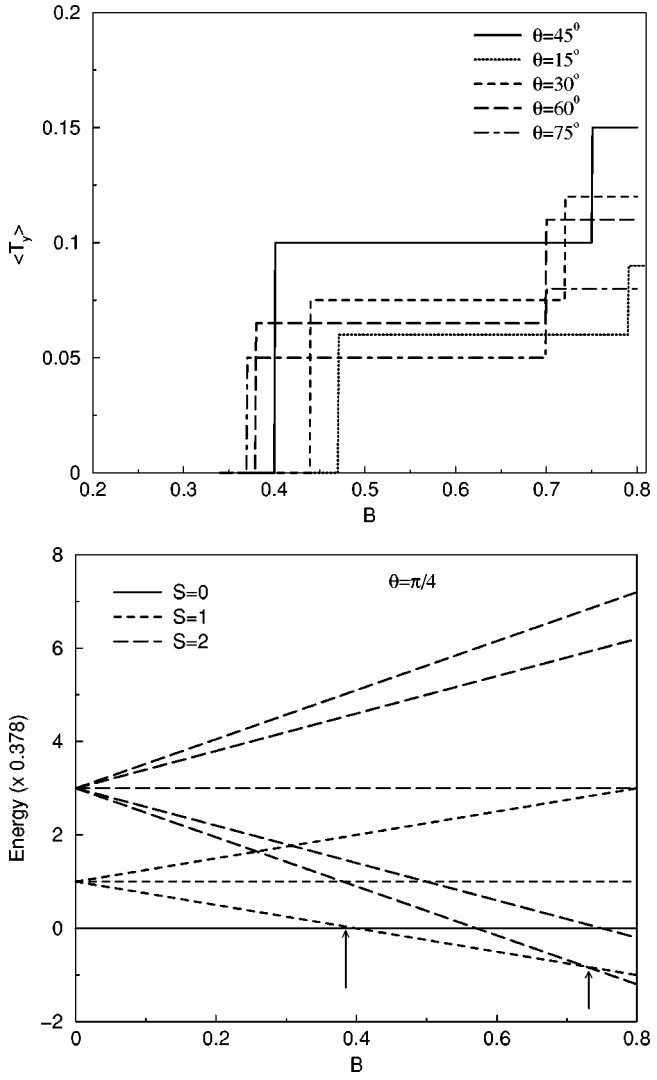

FIG. 8. (a) Plot of the $\hat{y}$ component of torque (in units of $J/\hbar$ rad) with change in magnetic field for different directions θ in the x-z plane. (b) Plot of energy levels corresponding to different spin states as a function of magnetic field at $\theta = \pi/4$. Note that the jump in the torque occurs at the field values where there is a change in the M_s value of the ground state.

tization oscillates with a low frequency and that the upper envelope of the curve Ω/ω versus H_0 behaves as $\sqrt{p} \sim 1/\sqrt{H_0}$.[14]

This nontrivial variation of Ω with H_0 can be understood from the viewpoint of Floquet's theorem.[23] Nonadiabatic transitions are possible whenever any two energy levels of a system are close to crossing, which, in our model, occurs whenever $\cos(\omega t)$ is close to zero. For these times, the two states with different magnetizations are nearly degenerate, leading to large tunneling amplitudes between the states which are manifested in oscillations of the magnetization. This magnetization oscillation can be related to that of macroscopic quantum coherence, which is predicted by Zvezdin.[20]

C. Torque magnetometry

Cornia *et al.* have used a novel cantilever torque magnetometry technique to study the spin-state crossover in ferric wheels. The torque **T** experienced by a magnetically anisotropic substance in a uniform magnetic field **B** is given by

$$\mathbf{T}=\mathbf{M}\times\mathbf{B}, \tag{14}$$

where **M** is the magnetization of the sample. **T** vanishes when the magnetic field is applied along one of the principle directions $\hat{x}$, $\hat{y}$, $\hat{z}$ of the susceptibility tensor, since in this case **M** and **B** are collinear. The $\hat{y}$ component of the torque operator, $\mathbf{T}_y$, can be easily obtained for an applied magnetic field of the form

$$\mathbf{B}=B(\cos\theta\hat{z}+\sin\theta\hat{x}), \tag{15}$$

in Eq. (5), and is given by

$$\langle\mathbf{T}_y\rangle=-g\mu_B B(\langle S_x\rangle\cos\theta-\langle S_z\rangle\sin\theta), \tag{16}$$

where $\langle S_\alpha\rangle=\Sigma_{i=1}^{N}\langle S_{i,\alpha}\rangle$ is the ground-state expectation value of the component α of the total spin operator.

From the structure of the Hamiltonian in Eq. (5), we see that the susceptibility tensor is diagonal and has the form $\chi_{ii}=(\alpha,\beta,\gamma)$ for $i=x,y,z$, with $\alpha\approx\beta\ll\gamma$. This implies that for an applied field of the form given in Eq. (15), $\vec{M}$ takes the form $B(\gamma\cos\theta\hat{z}+\alpha\sin\theta\hat{x})$. Hence $\langle\mathbf{T}_y\rangle\sim B(\gamma-\alpha)\sin\theta\cos\theta$, which has a maximum at $\theta=\pi/4$. If on the other hand, had we chosen $\vec{B}=B(\cos\theta\hat{x}+\sin\theta\hat{y})$ lying in the x-y plane, then $\vec{M}$ would take the form $B(\alpha\cos\theta\hat{x}+\beta\sin\theta\hat{y})$, and $\langle\mathbf{T}_z\rangle$ would be of the form $B(\alpha-\beta)\sin\theta\cos\theta$. Since $\alpha\approx\beta$, this would be much smaller in magnitude than for a field in the x-z plane, although the θ dependence would be similar.

We have computed $\langle\mathbf{T}_y\rangle$ for Fe_{12} on the basis of the eigenvectors of the Hamiltonian in Eq. (5). In Fig. 8(a), we have shown the variation of $\langle\mathbf{T}_y\rangle$ with the magnetic field for various values of θ, and we do observe a maximum in $\langle\mathbf{T}_y\rangle$ for $\theta=\pi/4$. We can clearly observe the step behavior of the torque component which is a manifestation of the level crossing of singlet, triplet, and quintet states. The fields at which the torque shows a jump are also seen to coincide with fields at which the M_s value of the ground state changes abruptly as indicated in Fig. 8(b).

IV. SUMMARY AND OUTLOOK

We have implemented a general and efficient procedure that allows us to block-factorize the spin Hamiltonian matrix based on its invariance under cyclic symmetry and parity operations. This method can be used in general for systems of other symmetries also. We have obtained the low-lying eigenvalue spectrum of ferric wheels up to Fe_{12} using the C_n rotational symmetry of the molecules. We have also analyzed the dispersion spectrum and structure factor. To reproduce the low-temperature properties of ferric wheels, we need to know the low-lying eigenvalue spectrum of these systems. We have also studied the dynamics of the ferric wheel by evolving an initial state whose magnetization is directed opposite to the direction of the magnetic field. We observe a nontrivial oscillation of magnetization in the presence of an alternating magnetic field. We have also obtained the torque of the ferric wheels in the presence of a nonaxial magnetic field and find that the torque also exhibits a steplike behavior with field. Evidently a study including the effect of nonzero temperature on this oscillation is a challenging problem for future research.

ACKNOWLEDGMENT

We thank CSIR, India, and DAE-BRNS, India, for financial support.

[1] K. L. Taft, C. D. Delfs, G. C. Papaefthymiou, S. Foner, D. Gatteschi, and S. J. Lippard, J. Am. Chem. Soc. **116**, 823 (1994).

[2] G. L. Abbati, A. Cornia, A. C. Fabretti, and W. Malavasi, Inorg. Chem. **36**, 6443 (1997); A. Caneschi, A. Cornia, and S. J. Lippard, Angew. Chem. Int. Ed. Engl. **4**, 467 (1995); K. L. Taft and S. J. Lippard, J. Am. Chem. Soc. **112**, 9629 (1990); R. W. Saalfrank, I. Bernt, E. Uller, and F. Hampel, Angew. Chem. **109**, 2596 (1997); A. Caneschi, A. Cornia, A. C. Fabretti, and D. Gatteschi, Angew. Chem. Int. Ed. Engl. **38**, 1295 (1999).

[3] J. C. Bonner and M. E. Fisher, Phys. Rev. **135**, A640 (1964).

[4] F. D. M. Haldane, Phys. Lett. **93A**, 464 (1983); Phys. Rev. Lett. **50**, 1153 (1983); I. Affleck, J. Phys.: Condens. Matter **1**, 3047 (1989).

[5] D. Gatteschi and L. Pardi, Gazz. Chim. Ital. **123**, 231 (1993).

[6] O. Waldmann, R. Koch, S. Schromm, J. Schülein, P. Müller, I. Bernt, R. W. Saalfrank, F. Hampel, and E. Balthes, Inorg. Chem. **40**, 2986 (2001); O. Waldmann, Phys. Rev. B **61**, 6138 (2000).

[7] Juan Bruno and R. J. Silbey, J. Phys. Chem. A **104**, 596 (2000).

[8] A. Cornia, A. G. M. Jansen, and M. Affronte, Phys. Rev. B **60**, 12 177 (1999).

[9] M. H. Julien, Z. H. Jang, A. Lascialfari, F. Borsa, M. Horvatic, A. Caneschi, and D. Gatteschi, Phys. Rev. Lett. **83**, 227 (1999).

[10] M. Affronte, J. C. Lasjaunias, A. Cornia, and A. Caneschi, Phys. Rev. B **60**, 1161 (1999).
[11] M. Enz and R. Schilling, J. Phys. C **19**, L711 (1986); **19**, 1765 (1986); J. L. Van Hemmen and A. Suto, Europhys. Lett. **1**, 481 (1986); E. M. Chudnovsky and L. Gunther, Phys. Rev. Lett. **60**, 661 (1988).
[12] A. Chilero and D. Loss, Phys. Rev. Lett. **80**, 169 (1998).
[13] B. Normand, X. Wang, X. Zotos, and D. Loss, Phys. Rev. B **63**, 184409 (2001).
[14] S. Miyashita, K. Saito, and H. De Raedt, Phys. Rev. Lett. **80**, 1525 (1998).
[15] A. Caneschi, D. Gatteschi, C. Sangregorio, R. Sessoli, L. Sorace, A. Cornia, M. A. Novak, C. Paulsen, and W. Wernsdorfer, J. Magn. Magn. Mater. **200**, 182 (1999).
[16] For a review, see S. Ramasesha and Z. G. Soos, in *Valence Bond Theory and Chemical Structure*, edited by D. J. Klein and D. L. Cooper (Elsevier, Amsterdam, in press).
[17] S. Ramasesha and Z. G. Soos, J. Chem. Phys. **98**, 4015 (1993).
[18] E. R. Davidson, J. Comput. Phys. **17**, 87 (1975).
[19] E. Lieb, T. Schultz, and D. Mattis, Ann. Phys. (N.Y.) **16**, 407 (1961); E. Lieb and D. Mattis, J. Math. Phys. **3**, 749 (1962).
[20] A. K. Zvezdin, cond-mat/0004074 (unpublished).
[21] It is also possible to observe the dynamics by starting with the ground state $|G\rangle$ of Eq. (5) as the initial state which has a large overlap with the state $|S=1,M_S=-1\rangle$. $|G\rangle$ is obtained by applying a large constant magnetic field B_0 in Eq. (5). The dynamics of the magnetization $M(t)$ is followed by evolving $|G\rangle$, using the field $h(t)$ in Eq. (6), after setting $B_0=0$. This is equivalent to shifting the chemical potential to induce a magnetization in the ground state.
[22] J. des Cloizeaux and J. J. Pearson, Phys. Rev. **128**, 2131 (1962).
[23] J. H. Shirley, Phys. Rev. **138**, B979 (1965).